

## A Poroelastic Analysis to Address the Impact of Depletion Rate on Wellbore Stability in Openhole Horizontal Completions

*Salam P. Salamy, Saudi Aramco, Thomas Finkbeiner, GeoMechanics International, Inc.*

Copyright 2000, ADIPEC

This paper was selected for presentation at the 10<sup>th</sup> Abu Dhabi International Petroleum Exhibition and Conference held in Abu Dhabi, U.A.E., 13-16 October 2002.

This paper was selected for presentation by ADIPEC Program Committee following review of information contained in an abstract submitted by the author(s). Contents of the paper, as presented, have not been reviewed by ADIPEC and are subject to correction by the author(s). The material, as presented, does not necessarily reflect any position of the ADIPEC or its members. Permission to copy is restricted to an abstract of not more than 300 words; illustrations may not be copied. The abstract should contain conspicuous acknowledgment of where and by whom the paper was presented. Write ADIPEC Secretary, GEC, P. O. Box 5546, Abu Dhabi, UAE, Fax 009712-4446135.

### Abstract

This paper highlights the development of a coupled poroelastic geomechanical and fluid flow model which incorporates field and lab data with the objective to constrain the full in-situ stress tensor and rock strength in order to predict the stability of open hole horizontal completions during reservoir depletion.

Results of a four-year comprehensive testing and monitoring program conducted to assess the extent of hole instability during shut-in and flowing periods<sup>1</sup> indicated that there was no immediate hole collapse. However, the study revealed the need to assess the long-term impact of reservoir depletion and pressure drawdown on wellbore stability.

The results of this study indicate that the in situ stress state can be characterized by a normal faulting environment with low differential stresses in which the maximum principal stress is approximately equal to the overburden. Furthermore, a detailed analysis of wellbore stability during production supports openhole completion for horizontal wells under the condition that reservoir depletion is limited to a maximum pressure drop of 1,500 psi. This finding is independent of well azimuth. Pressure drops exceeding 1,500 psi in the reservoir are likely to cause considerable wellbore instabilities. These results were achieved under the assumption of moderate to more pronounced amounts of drawdown (500-1000 psi) in the near wellbore region. The study also highlighted that laboratory-derived rock strength values from triaxial tests, are low and are not consistent with the drilling and production experiences to date in the field. Rather, the formation appears to behave in a plastic manner that strengthens the wellbore.

### Introduction

Hole stability concerns in the Shu'aiba reservoir, Shaybah Field, Saudi Arabia, first surfaced during the drilling and logging of two development vertical evaluation/production wells where a logging tool was stuck in one well due to tight hole, and indications of tight hole were encountered while drilling another well. The two incidents signaled the need to investigate hole stability in the Shu'aiba reservoir.

A review of all the vertical delineation wells drilled in the

1960's for problems associated with hole fill and/or collapse during drilling and production found no conclusive evidence for stability problems.

Cores taken in the mud-rich, high porosity rock of the Shu'aiba formation have been described as having a "toothpaste-like" texture and behavior. Preliminary laboratory rock mechanics studies indicated that the Shu'aiba carbonates are mechanically weak with the majority of the rocks tested yielding very low strength values (less than 2000 psi) when compared to samples from other carbonate reservoirs.

In light of the gathered field and geomechanics data, a comprehensive hole stability monitoring program was formulated and initiated with the objective to investigate the extent and implications of hole stability on field development and deliverability. Results of which are summarized in SPE 56508<sup>1</sup> indicating, at least in the short term, no impact of production on wellbore stability.

Furthermore, a long term study, which is the focus of this paper, was initiated to constrain the full in situ stress tensor (i.e., orientation and magnitude), reservoir pore pressure, and rock strength in order to build a geomechanical model of the Shaybah Field and predict the stability of openhole horizontal wells during reservoir depletion. To achieve these goals, a broad suite of available data from wells drilled in Shaybah Field were utilized such as electrical FMI image data, four-arm caliper logs, minifrac, wireline logs (e.g., density, neutron, and sonic logs), and pore pressure information obtained by direct measurement were studied. This data—sufficient to constrain the full stress tensor and pore pressure—was then augmented by information on uniaxial compressive strength derived from laboratory measurements and log data to build the full geomechanical model, which was then used as a basis to predict wellbore stability during reservoir depletion.

### Background

**Field History.** The Shaybah field discovered in 1968, in the Ruba Al-Khali desert of Saudi Arabia, is approximately 8 miles (13 kilometers) wide and 40 miles (64 kilometers) long (Figure 1). The surface terrain is comprised of flat sabkhas and mountainous sand dunes (up to 200 meters tall). Because of its rugged and unstable character, the field is developed from the flat sabkhas necessitating highly directional and horizontal drilling to reach the targets.

The oil in Shu'aiba formation is Arabian Extra Light with an average API of 42°. The oil in Shu'aiba reservoir is overlain by a huge gas cap and underlain by a water aquifer. 3-D seismic data show that the Shu'aiba reservoir has a number of faults. These faults and fractures have also been identified from logs and formation evaluation and their presence makes the field more prone to gas or water coning.

**Shaybah Geology and Tectonic Setting.** At the depth, the Shaybah field is characterized as a gently folded northeast-southwest trending anticline consisting primarily of cretaceous age sandstones, shales, and carbonates. The reservoir is the Early Cretaceous Shu'aiba Formation. The carbonate Shu'aiba Formation consists of ruddist build-ups that vary laterally into barrier and shelf slope facies. While porosity is generally high and does not vary laterally; permeability is facies-dependent and varies laterally and vertically. The Shu'aiba Formation conformably overlies the carbonate Biyadh Formation. The Shu'aiba is overlain by the middle Cretaceous Khafji or Nahr Umr Shale, a member of the Wasia Formation, which acts as a seal. The contact between the Shu'aiba and Nahr Umr Shale is a non-depositional and possibly erosional unconformity<sup>2</sup>.

**Wellbore Failure from Time-Lapse Caliper.** Saudi Aramco carried out a systematic study of changes in wellbore size over time during periods of shut-in and production. A short caliper campaign was conducted in April 1997 prior to field startup in which a caliper log was run in four horizontal wells. The reservoir was subsequently produced at maximum rates for approximately two to four weeks and then a second caliper was run. Caliper data from two additional horizontal wells were recorded in December 1997 and June 1998. Caliper data from all the six wells were recorded in December 1998 and December 1999. Details of the caliper campaign, testing and monitoring campaigns, data analysis and results are summarized in SPE paper 56508<sup>1</sup>.

A review of caliper data showed no evidence of developing breakouts or borehole collapse over time even though gradual shape changes were observed in the wells. These shape changes generally showed an effective hole enlargement from smaller than bit size to approximately equal to bit size. These changes were probably due to the removal of unusually thick mud cake (due to the polymer mud used during drilling), accumulated debris at the bottom of horizontal boreholes, or plastic deformation (i.e., creep).

### Constraining Stress Orientation

**Wellbore Failure Analysis.** Electrical (FMI) and mechanical four arm caliper data from six vertical wells and eight horizontal wells (i.e., a total length of 30,613 feet or 9,331 meters) were analyzed in order to identify stress-induced wellbore failure such as breakouts and tensile fractures. Wellbore breakouts are enlargements of the wellbore wall with 180° spacing caused by shear failure where the circumferential hoop stress is most compressive and when it exceeds the compressive strength of the rock.

In vertical wells, breakouts always form in the direction of the least principal horizontal stress ( $S_{hmin}$ )<sup>3,4</sup> and tensile fractures always in the direction of the maximum principal horizontal stress ( $S_{Hmax}$ )<sup>5</sup>. In deviated wells however, the position of breakouts in a well is a function of the wellbore trajectory and the stresses acting on the well<sup>6</sup>. Therefore, when wellbore failures can be detected, their occurrence and characteristics can be used to constrain in-situ stress magnitudes, effective rock strength, and stress orientations.

**Electrical Image Data.** Most of the FMI images acquired in intervals of the Shu'aiba limestone were of low quality (due to the build up of unusually thick mud cake), and therefore prevented the detection of wellbore failure. In the remaining, better quality intervals, no conclusive evidence of stress-induced wellbore failure was identified.

**Four Arm Caliper Data.** In caliper data, breakouts must be distinguished from other stress-induced or drilling-induced enlargements such as washouts and keyseats. Failure to utilize strict criteria for breakout identification can result in the misinterpretation of washouts and keyseats as wellbore breakouts. For this analysis the criteria defined by Plumb and Hickman<sup>7</sup> were utilized.

The initial caliper analysis focused on data in the shale units above the Shu'aiba Reservoir. Because the horizontal wells were logged with a fixed tool orientation, only the vertical wells could be analyzed. Three vertical wells, all located in the northern part of the field, qualified for this analysis. Enlargements were detected in two of the three wells and their orientations are shown as rose diagrams in Figure 2. Enlargements in one well have a bimodal distribution with azimuths in east-northeast-west-southwest and east-southeast-west-northwest orientations (Figure 2a). Enlargement azimuths in the other well have an east-west orientation (Figure 2b). In the third well, both calipers are less than bit size, therefore, no enlargements were detected.

Since breakouts were not observed in the FMI image data of the two wells where the caliper data indicate enlargements, it is possible that the enlargements are so severe that opposing tool arms may be completely recessed into breakouts.

Caliper analysis was also performed in the Shu'aiba limestones of six vertical wells. In two of the wells, pad 1 azimuth is continuously rotating, indicating that the hole is in-gauge. In the four other wells, the caliper diameters frequently fall below bit size, suggesting the presence of mud cake build-up. Only a small number of enlargements were detected in one of these four wells, that may qualify as stress-induced breakouts. The enlargements in this well show a bimodal azimuth distribution with the dominant population having a northeast-southwest orientation and the secondary population having a north-northeast-south-southwest orientation (Figure 3). Unfortunately, most of the FMI data in these intervals are of poor quality, so the nature of these wellbore enlargements cannot be determined from the images.

The majority of the breakouts detected in the caliper data analysis have a mean orientation of east-west. Since the wells in which these breakouts were detected are vertical, the azimuth of  $S_{Hmax}$  is approximately north-south.

### Determination of Rock Strength

Determination of rock strength—in particular, uniaxial compressive rock strength,  $C_0$  (also referred to as UCS)—is critical to understand wellbore stability during drilling and production and is utilized for constraining the full in situ stress tensor. In this section, we discuss two methods that we used to determine uniaxial rock strength for the formations of the Shaybah Field.

### Rock Strength from Laboratory Measurements.

Compressive strength data from triaxial laboratory tests were compiled to determine uniaxial compressive strengths for the Shu'aiba Formation<sup>8</sup>. The triaxial tests were conducted by applying multiple and successively higher confining pressures to an individual sample and testing it in each cycle to a perceived onset of failure. In other words, complete failure indicating the loss of cohesion was not achieved in these tests. As shown below, this multi-stage triaxial testing procedure seems to yield systematically low values of  $C_0$ .

Figures 4 and 5 show histograms of  $C_0$  and  $\mu_i$  as derived from the lab measurements. The results reveal a wide range of  $C_0$  values (i.e., from about 2 MPa to 34 MPa with a mean value of  $12.5(\pm 7.1)$  MPa). This low mean value for  $C_0$  indicates a weak Shu'aiba Formation. However, associated low  $\mu_i$  values may imply that the samples had already failed at low confining pressures and the failure at higher confining pressures is simply the result of sliding along pre-existing shear planes. This failure along pre-existing failure planes may also be responsible for low peak stresses at failure. Hence, resulting compressive strength values would then represent lower bound value for  $C_0$ . Alternative explanations for the low strength and friction values could be that the specimens were not tested all the way to brittle shear failure, that the samples had degraded before testing due to dessication, or that plastic (i.e., shear-enhanced compaction and internal porosity reduction) rather than brittle deformation governed the specimens failures. This latter process can actually strengthen the specimens rather than bring them to failure revealing that the tested strength values are again effectively lower bounds to the uniaxial rock strength of the Shu'aiba Formation.

**Deriving Rock Strength from Well-Log Data.** An alternative approach for deriving uniaxial compressive rock strength is by the evaluation of petrophysical and well-log data. For this purpose, we selected a vertical well with the most complete suite of well-logs (i.e., gamma ray, neutron porosity, and bulk density) and applied a proprietary relationship that relates effective porosity versus strength. This relationship was calibrated to the appropriate lithology encountered in the well through a large database of laboratory-derived strengths.

Figure 6 displays the resulting continuous strength log as a function of depth and, for comparison, the discrete  $C_0$  values derived from the laboratory measurements discussed above. The  $C_0$  log indicates a range of  $C_0$  values from approximately 25 MPa to 65 MPa. The  $C_0$  values derived from the laboratory measurements consistently under-predict the log-derived strength values by up to 45 MPa. While we discussed potential problems with the procedure of the laboratory measurements and the resulting strength values above, we do not believe that these problems can account for a difference in rock strength to the strength log values by an order of magnitude. This relatively large difference in strength values between the two methods suggests, as discussed above, that there are pre-existing flaws or degradation processes that had weakened the samples before the laboratory testing even started. In

addition, plastic deformation may have strengthened the rocks in situ around the wellbore resulting in an even wider discrepancy between the  $C_0$  values derived through the two methods discussed.

For the purposes of this study, the strength values obtained from the laboratory measurements and the log transform were used as lower and upper bounds, respectively. However, it appears as if the strength values from the log transform are somewhat more accurate in order to be consistent with the general absence of wellbore failure and drilling experience. Had the uniaxial compressive strength been as low as that suggested by the lab measurements, wellbore failure would have probably been severe, yet this was not observed.

### Pore Pressure

Pore pressure ( $P_p$ ) can be determined using a variety of techniques including direct measurement and inference from mud weight and logging data. In the Shaybah Field a number of results from both direct and indirect sources were utilized to constrain pore pressure as a function of depth. Direct pore pressure measurements (i.e., DST, MDT, measurement during a minifrac tests, etc.) were made in six wells. Figure 7 shows these measurements (blue squares) as a function of true vertical depth. The results from the MDT further provided estimates of hydrocarbon density that were used to calculate pore pressures above and below the measurement depth. The pore pressure gradient determined from the MDT is 0.28 psi/ft for oil and 0.47 psi/ft for water (brine). Pore pressures within the oil and water columns are calculated using the respective gradients and assuming the reservoir is in static equilibrium.

Further constraints were placed on the pore pressure by comparing the mud weights utilized during drilling with observations of formation losses or unexpected fluid production. Ten wells provided this information. Wells that showed unexpected production are assumed to have mud weights below the formation pressure. In these cases, the recorded mud weight is assumed to be a lower bound for the pore pressure (right pointing triangles, Figure 7). Wells that showed circulation losses are assumed to have mud weights above the formation pressure. In these cases, the recorded mud weight is assumed to be an upper bound for the pore pressure (left pointing triangles in Figure 7).

Overall, the results indicate that pore pressure is close to hydrostatic (i.e., pore pressure follows a gradient of approximately 0.45 psi/ft) to a depth of approximately 4,600 feet, where  $P_p$  appears to increase. In the Shu'aiba Reservoir, at depths between approximately 4,750 feet and 5,000 feet, measurements reveal that pressures are in excess of hydrostatic. The maximum pressure measured in this reservoir is approximately 2,450 psi at 4,900 feet, which is 245 psi above the hydrostatic pore pressure. A measurement at 6,473 feet indicates the pore pressure is again hydrostatic at greater depth (Figure 7).

### Stress Magnitudes

**Overburden.** The overburden stress (i.e., vertical stress,  $S_v$ ) profile was calculated through integration of density logs in five wells. All wells showed similar results over the

sampled depth ranges, including a significant increase in density from approximately 1,200 feet to 2,200 feet. The average overburden gradient is approximately 1.03 psi/ft at the reservoir level (Figure 7).

**Minimum Principal Stress.** The minimum principal stress ( $S_3$ ) was determined from minifracs conducted in three wells. In two wells the instantaneous shut-in pressure (ISIP) was picked from the pressure-time curve as the minimum principal stress. The values of the minimum principal stress determined from the ISIP were 4,195 psi and 3,950 psi (Figure 7). Because no pressure-time data were available for the third well, the reported fracture closure pressure (FCP) was used as the minimum principal stress. The FCP is 4,100 psi, which is consistent with the estimates of  $S_3$  obtained in the previous two wells. The resulting least principal stress gradients range from 0.79 psi/ft to 0.84 psi/ft and are all well below the vertical stress. Hence, the minimum principal stress ( $S_3$ ) must by definition be the minimum horizontal stress ( $S_{hmin}$ ) in the Shaybah Field.

**Maximum Principal Stress.** To constrain the maximum horizontal stress ( $S_{Hmax}$ ), stress polygons plotting  $S_{Hmax}$  versus  $S_{hmin}$  magnitudes were constructed at a single depth (Figure 8). A stress polygon illustrates all possible in situ stress states<sup>5</sup>. The perimeter of the polygon indicates the limiting values of  $S_{hmin}$  and  $S_{Hmax}$  for which the state of stress is in equilibrium with the frictional strength of pre-existing faults, as predicted by Coulomb faulting theory<sup>9</sup>. Stress states within the polygon correspond to normal faulting (NF:  $S_v > S_{Hmax} > S_{hmin}$ ), strike-slip faulting (SS:  $S_{Hmax} > S_v > S_{hmin}$ ), or reverse faulting (RF:  $S_{Hmax} > S_{hmin} > S_v$ ) stress states in which the ratio of shear to effective normal stress on any arbitrarily oriented fault is less than the coefficient of sliding friction ( $\mu_f$ , commonly 0.6–1.0). Furthermore, to constrain a stress state consistent with in situ conditions and observations of wellbore failures, the stress polygon is constructed for the mud weights used during drilling and the observed pore pressure conditions. Finally, contour lines of rock strength are superimposed on the stress polygon to take into account the occurrence (or absence) of wellbore breakouts. The strength values plotted on the contour lines reflect the  $C_0$  values from the strength log at a depth for which the stress polygon was constructed. This approach was described in detail by Peska and Zoback<sup>6</sup>.

Stress polygons were constructed in several wells to constrain  $S_{Hmax}$  magnitudes at depths where breakouts were both observed and not observed. This approach allows to place upper and lower bounds on  $S_{Hmax}$ . Figure 8 presents an example of this stress polygon, which was constructed for the Shu'aiba reservoir where no breakouts were observed. At this depth, the strength log predicts rock strength values between 5,300 psi and 6,500 psi. However, laboratory-derived rock strengths indicate an average strength of approximately 2,000 psi. Hence, stress magnitudes are required to be below the appropriate sub-horizontal rock strength contour in order for the model to predict that breakouts should not be observed. The box inside the polygon shows the likely range of minimum

horizontal stress values determined at this depth (3,950 to 4,195 psi). This result suggests that the rock strength can in fact be no less than approximately 2,800 psi if the model is to remain consistent with the observations; otherwise, wellbore failure would have been observed. Therefore, we utilize the values from the strength log to place constraints on the upper bound of the maximum horizontal stress. These results show that  $S_{Hmax}$  cannot be much larger than  $S_v$  and, in fact, is likely to be significantly less.

Figure 7 shows the resulting upper and lower bound values of the maximum horizontal stress (with diamonds and arrow) from the stress polygon methodology. We further display in the figure values of the minimum horizontal stress and overburden determined previously. The results from this stress analysis indicates that the Shaybah Field is in a normal faulting stress state (that is:  $S_v \geq S_{Hmax} > S_{hmin}$ ). While there is some uncertainty in the estimates of  $S_{Hmax}$ , it is clear that  $0.82 \text{ psi/ft} \leq S_{Hmax} \leq 1.03 \text{ psi/ft}$ . Our estimate of the stress field is thus:

$$S_{hmin} \cong 0.82 \pm 0.2 \text{ psi/ft}$$

$$S_{Hmax} \cong 0.9 \pm 0.1 \text{ psi/ft}$$

$$S_v \cong 1.03 \pm 0.01 \text{ psi/ft}$$

These results indicate there is relatively little horizontal stress anisotropy in the Shaybah Field. Furthermore, the stress state is not in an incipient state of failure, in which optimally oriented pre-existing faults would be close to frictional slip.

### Dynamic Wellbore Stability

**Methodology and Input Data.** Important prerequisites for investigating wellbore stability are knowledge of the in situ state of stress, pore pressure, and uniaxial compressive rock strength. This is because circular wellbores strongly amplify the in situ stress state. Compressive rock failure around the borehole is a function of effective stresses, in situ rock strength, pore pressure in the formation, and pressure in the wellbore. Previous sections described the analysis of these parameters. A proprietary program uses this information to determine the zone of instability around the wellbore's circumference (i.e., the azimuthal width that is likely to fail) as a function of various parameters (e.g., pore pressure, rock strength). The program allows the choice of seven different rock failure criteria; these determine the exact size of failure at the wellbore wall depending on the underlying constitutive law and parameterization of rock strength. However, for all failure criteria, the initial zone of failure at the wellbore wall is quite similar and the range of required rock strength values is rather narrow. In this study, we exclusively used the Mohr Coulomb failure criterion—although had other failure laws been used, the overall quantitative results would not have been markedly different.

The orientation of the maximum principal horizontal stress was determined above to be approximately north–south. The pore pressure in the reservoir is 2,475 psi. The upper and lower bound estimates of  $S_{Hmax}$  are used to create two end member stress models at a depth of 4,950 feet. In the first model, the horizontal stresses are approximately equal and the vertical stress is the maximum principal stress. In the second model,  $S_{Hmax}$  is slightly greater than the vertical

stress. Table 1 summarizes the exact values used for each of the two models.

An approximate value for the compressive rock strength in the reservoir section was determined from the strength log to be approximately 7,250 psi. Rock strength tests indicate the rock strength is approximately 2,000 psi.

The average values for Young's modulus and Poisson's ratio determined from the rock strength tests are  $1.36 \times 10^6$  psi and 0.26, respectively. Average porosity and permeability for the Shu'aiba Reservoir are 24 % and 15 mD, respectively. Coefficients of sliding friction ( $\mu_f = 0.6$ ) and internal friction ( $\mu_i = 1.0$ ) were obtained from experience in similar fields throughout the world.

**Approach to Wellbore Stability Analysis.** The general approach followed in this study was to investigate the stability of horizontal wells drilled both parallel and perpendicular to the overall reservoir structure. The structure has a long-axis orientation of approximately N30°E. For each of these two families of wells two cases of drawdown: minor (i.e., 500 psi) and major (i.e., 1,000 psi) were considered. The minimum rock strength required to maintain stable borehole conditions was determined for time-dependent drawdown achieved after 100 minutes from the onset of production. A total of five scenarios with different pore pressure conditions in the reservoir were considered. Reservoir conditions in the first set were unaffected by production (i.e., undepleted,  $P_p = 2,475$  psi), while the second set considers reservoir depletion by 500 psi (i.e.,  $P_p = 1,975$  psi) and associated horizontal stress changes. In other words, as the reservoir pressure declines due to production, the horizontal stresses decline as well. These stress changes are calculated by assuming poroelastic reservoir behavior by which the effective horizontal stresses in the reservoir rocks increase in response to the reduced pore fluid pressure. This poroelastic model is two-dimensional and assumes a relatively flat, extensive (i.e., length  $\gg$  width) reservoir with constant overburden stress. For the horizontal principal stress changes, two cases were considered: 1) strong coupling between pore pressure and total stress (i.e., weak rock) with  $dS/dP = 0.75$  and 2) intermediate coupling with  $dS/dP = 0.5$ . The remaining three sets of scenarios assumed reservoir depletions of 1,000 psi, 1,500 psi, and 2,000 psi corresponding to pore pressures of 1,475 psi, 975 psi, and 475 psi, respectively. The calculated associated horizontal stress changes use the same two poroelastic parameters.

The reservoir depth and data limitations constrained our depth of focus to 4,970 feet. In each case a poroelastic analysis was applied to assess the time-dependent required rock strength as a function of drawdown in order to keep the borehole stable. Figure 9 shows an example output plot from this analysis. The plot exhibits color-coded rock strength values in the near wellbore region required to maintain borehole stability. Negative values have no physical meaning and indicate a stable region. The black line in the figure follows the contour for a  $C_0$  value of either 7,250 psi or 2,000 psi, depending on the model being run. The inside region defined by this contour indicates where the required rock strength exceeds the expected rock

strength and the wellbore wall is unstable since a stronger rock is required.

Figure 9 indicates that a drawdown of 500 psi achieved in 100 minutes would result in the development of  $\sim 100^\circ$ -wide breakouts at the sides of the well if the rock strength was as low as 2,000 psi. Under these conditions, the well would be highly unstable and open hole completion not advisable. The figure further demonstrates that  $C_0$  needs to be at least as high as 5,000 psi in order to reduce breakout width to approximately  $60^\circ$  (shown as dashed lines). According to the stability criteria further outlined below, breakouts of this width still have a sufficiently intact section (i.e., arch support) around the wellbore circumference to prevent stability problems.

**Stability Classification.** Because of the varying in situ conditions and the uncertainty in the rock strength values, it is important to establish reliable classification criteria for borehole stability when analyzing the results in each case. For a borehole to be stable, wall failure does not need to be inhibited altogether. Rather, the development of borehole breakouts up to a certain maximum width can be permitted (see Figure 9). As long as there is a sufficiently intact section of the wellbore circumference, enough strength (i.e., arch support) is provided to accommodate the stress concentration around the well and prevent entire borehole collapse. The concept of achieving a controlled region of failure with a finite, maximum breakout width without sacrificing stability is based on our experience from many previous case studies. For each case, the width of the enlargement (i.e., breakout) as predicted by the program based on the rock strength was measured. The well is generally stable, transitional, or generally unstable if the width of the failed circumference is smaller than  $60^\circ$ , between  $60^\circ$  and  $90^\circ$ , or larger than  $90^\circ$ , respectively.

**Results.** The results of this analysis are listed in Table 2 and can be summarized as follows:

**Initial Conditions.** For initial conditions in which the horizontal stresses are isotropic and the vertical stress is the maximum principal stress, horizontal wellbores drilled in weak rocks (i.e., 2,000 psi) fall within the transitional stability range. If the stresses are such that the maximum horizontal stress is slightly greater than the vertical stress, then a horizontal wellbore drilled parallel to structure and drawn down by 500 psi will be transitionally stable. However, if the well is drilled perpendicular to structure or the drawdown is increased, then horizontal wells will be unstable. In stronger rocks (i.e., 7,250 psi), horizontal wells are stable under any conditions.

**Depleted I and Depleted II.** For the cases of 500-psi and 1,000-psi depletion, stronger rock is stable and weaker rock is unstable, regardless of the reduction in horizontal stresses, the wellbore orientation, or the drawdown.

**Depleted III.** For the case of 1,500-psi depletion, the weaker rock is unstable and the stronger rock is stable if the drawdown is 500 psi. If the drawdown is increased to 1,000 psi, then horizontal wellbores become transitionally stable, regardless of stress or wellbore orientation.

**Depleted IV.** For the case of 2,000-psi depletion, we find that the weaker rock is unstable and the stronger rock is

transitionally stable. Severe drawdown forces the stronger rock to become unstable in the case of weak coupling between the pore pressure and the stress (i.e.,  $dS/dP = 0.5$ ).

**General Aspects.** In addition to the various input parameters considered in this study (stress state, pore pressure, well trajectory, etc.), there are three general aspects of these calculations that directly impact our findings. First, a wide range of rock strength values were used. As explained previously, the results from the rock strength log more accurately reflect the in situ rock strength. However, the variability in rock strength throughout the field will have an effect on wellbore stability. Second, some degree of wellbore failure is permitted to occur and the analysis focuses on determination of the conditions under which failure would become extreme. This empirical stability criterion has been successfully used in a number of other reservoirs in different parts of the world. Finally, the overall conclusions about wellbore stability are based upon a fully coupled poroelastic analysis of stress and pore pressure around a well, not upon the calculations from an overly simplified elastic analysis, which tends to over-predict the degree of wellbore instability.

#### Impact on Testing Procedures

Log derived strength values of approximately 7000 psi for the Shu'aiba reservoir are likely to be the upper bound estimates; strength could in fact be lower. However, based on all the available field and caliper data from the horizontal wells, the rock strengths of the reservoir of approximately 2000 psi appear to be very low. Because of the critical importance of rock strength in predicting safe levels of depletion and drawdown, additional laboratory measurements are required. Additional laboratory measurements on Shu'aiba reservoir rocks were recommended to better characterize their mechanical behavior by defining and mapping out in detail brittle and plastic failure lines.

The additional laboratory testing should be carried out in two stages. The first stage comprises a series of tests under hydrostatic conditions to identify the pressures under which internal porosity reduction occurs. In other words, when the sample has reached its so-called end-cap and deforms plastically resulting in mechanical compaction. The second stage of tests should be conducted under triaxial conditions to define the exact shape of this end cap failure line.

#### Conclusions

To identify the impact of dynamic reservoir depletion on the stability of horizontal wellbores and the long term impact on completion strategy, a geomechanical model was constructed for the Shu'aiba Formation in the Shaybah Field. This model is based on measurements of in situ reservoir conditions and consistent with observations of wellbore failures derived from electrical image logs.

The in situ stress state can be characterized as a normal faulting environment in which the maximum horizontal principal stress is approximately equal to the overburden oriented N-S.

Rock strength values were derived from well log data, which are appreciably larger than lab-derived rock strength values. While experience to date is consistent with higher strength values highlighting that the rock is undergoing plastic compaction thereby strengthening the wellbores. Additional rock strength measurements addressing this phenomenon are underway.

The findings of the dynamic stability analysis can be directly interpreted with respect to the feasibility of utilizing horizontal wells and open hole completions in the Shu'aiba Reservoir. As summarized in Table 2, the numerical experiments demonstrate the following:

- For weaker rock (i.e.,  $C_0 = 2,000$  psi), horizontal holes may be unstable under initial conditions and are unstable under all depletion and drawdown scenarios.
- For stronger rock (i.e.,  $C_0 = 7,250$  psi), horizontal uncased wells are most stable when the drawdown is moderate (i.e., 500 psi). Severe drawdown (i.e., 1,000 psi) begins to cause wellbore instabilities when the depletion reaches 1,500 psi.
- In stronger rock under severe depletion (i.e., 2,000-psi depletion,  $P_p = 475$  psi), the wellbore is expected to become increasingly unstable regardless of the drawdown scenario.
- There is not a strong correlation between drilling direction and stability of horizontal holes.

#### Acknowledgments

The authors would like to extend their sincere gratitude and appreciation to Saudi Aramco management and Saudi Oil Ministry for permitting the publication of this effort. Special thanks are extended to Mr. A. M. Al-Ajmi, Mr. H. K. Al-Mubarak, Mr. J. Funk, and Mr. R. Sadler for their insights, and contribution to the study. Special thanks are extended to Shaybah Production Engineering for coordinating and executing the caliper campaigns and for the Saudi Aramco R&D Center for conducting the laboratory tests. The authors are also thankful to GeoMechanics International (GMI) for use of their proprietary software GMI•Imager™, GMI•SFIB™, and GMI•Caliper™ in this study

#### Nomenclature

$C_0$  = Uniaxial Compressive Rock Strength

$S_{hmin}$  = Least Principal Stress

$S_{Hmax}$  = Maximum Principal Stress

$P_p$  = Pore Pressure

MDT = Modular Dual Testing

$S_v$  = Vertical Stress

ISIP = Instantaneous Shut-in Pressure

NF = Normal Faulting

SS = Strike Faulting

RF = Reverse Faulting

#### References

1. Salamy, S.P., et al., 1999, "Methodology Implemented in Assessing and Monitoring Hole Stability Concerns in Open-hole Horizontal Wellbores in Carbonate Reservoirs". SPE, Annual Technical Conference, paper 56508, Houston, Texas.

2. Alfaraj, M., E. L. Nebrija, and M. D. Ferguson, 1998. The challenge of interpreting 3-D seismic in Shaybah Field, Saudi Arabia, *GeoArabia*, v. 3, pp. 209–226.
3. Gough, D. I., and J. S. Bell, 1981. Stress orientations from oil well fractures in Alberta and Texas, *Can. Jour. Earth Sci.*, v. 18, pp. 638–645.
4. Zoback, M. D., D. Moos, L. Mastin, and R. N. Anderson, 1985. Wellbore breakouts and in-situ stress, *J. Geophys. Res.*, v. 90, pp. 5,523–5,530.
5. Moos, D., and M. D. Zoback, 1990. Utilization of observations of well bore failure to constrain the orientation and magnitude of crustal stresses: Application to continental, Deep Sea Drilling Project and ocean drilling program boreholes, *J. Geophys. Res.*, v. 95, pp. 9,305–9,325.
6. Peska, P., and M. D. Zoback, 1995. Compressive and tensile failure of inclined well bores and determination of in situ stress and rock strength, *J. Geophys. Res.*, v. 100, no. 7, pp. 12,791–12,811.
7. Plumb, R. A., and S. H. Hickman, 1985. Stress-induced borehole elongation: a comparison between the four arm caliper dipmeter and the borehole televiewer in the Auburn geothermal well, *J. Geophys. Res.*, v. 90, no. 5, p. 513.
8. Lauten, W. T., J. J. Funk, and K. Merajuddin, 1997. Petrophysics Unit Mechanical Properties of Shu'aiba Carbonates, The Saudi Aramco Laboratories Research and Development Center, ARI 310-01/97, 22 pp., July 13.
9. Zoback, M. D., and J. H. Healy, 1992. In situ stress measurements to 3.5 km depth in the Cajon Pass scientific research drill hole: Implications for the mechanics of crustal faulting, *Jour. Geophys. Res.*, v. 97, no. 4, pp. 5,039–5,057.

**Figures**



Figure 1. Schematic map of the Shaybah Field with well locations from which data were available.

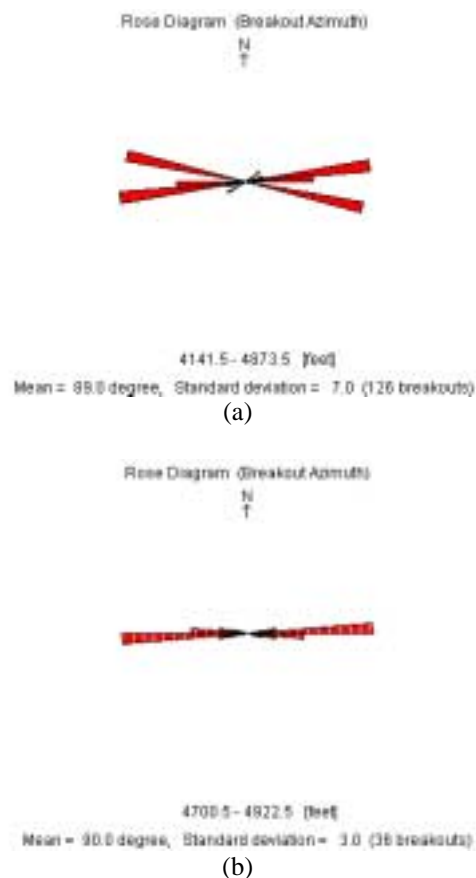


Figure 2. Rose diagrams of enlargement azimuths as observed in the shale units above the Shu'aiba reservoir.

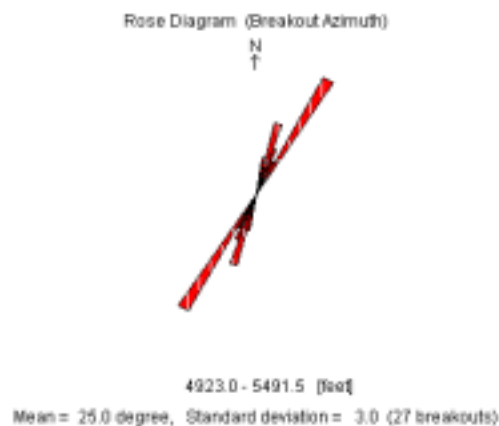


Figure 3. Rose diagram of enlargement azimuths in the Shu'aiba limestone.

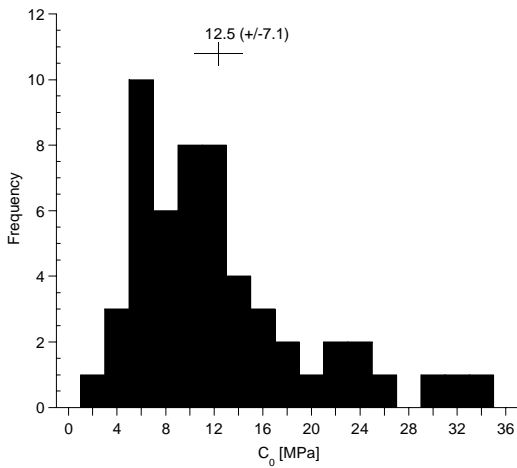


Figure 4. Histogram of  $C_0$  from the multi-stage tests on individual specimens. The mean strength is 12.5 ( $\pm 7.1$ ) MPa.

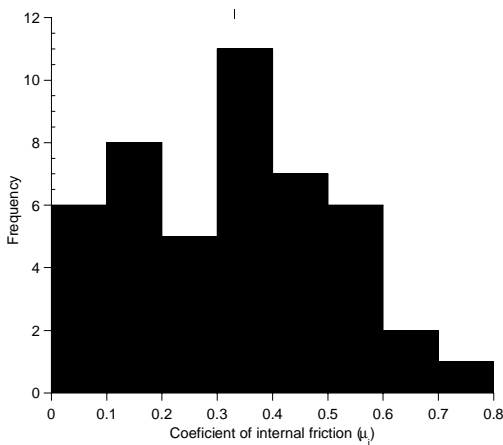


Figure 5. Histogram of  $\mu_i$  values. The mean value is 0.33 ( $\pm 0.19$ ).

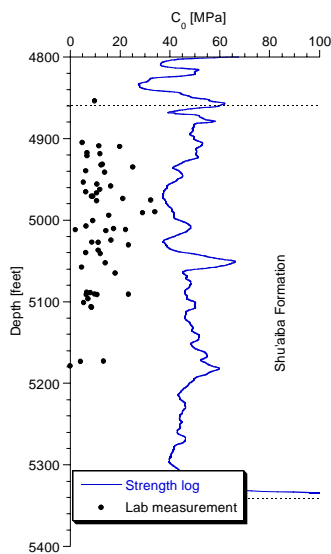


Figure 6. Unconfined compressive strengths ( $C_0$ ) derived from well-log data utilizing an effective porosity versus strength relationships and discrete  $C_0$  values from the triaxial multi-stage laboratory measurements.

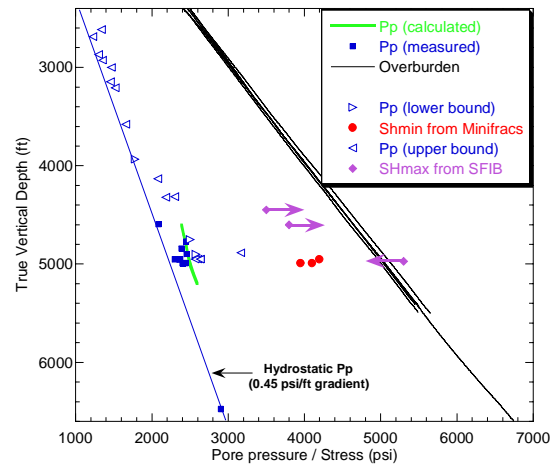


Figure 7. Stress and pore pressure as a function of depth in the Shaybah Field.

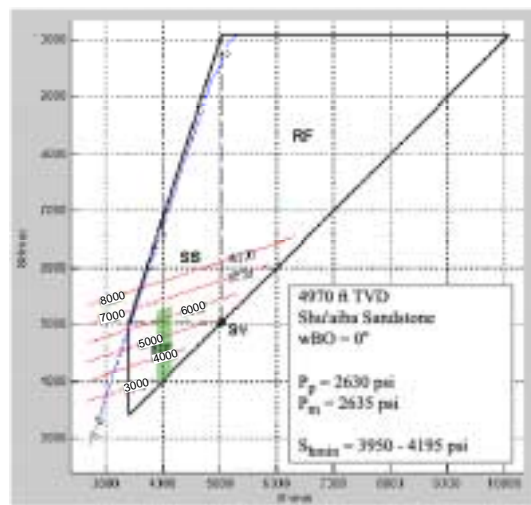


Figure 8. Stress polygon constructed for the Shu'aiba reservoir. The box outlines all possible combinations of  $Sh_{min}$  and  $SH_{max}$  consistent with the absence of breakouts.

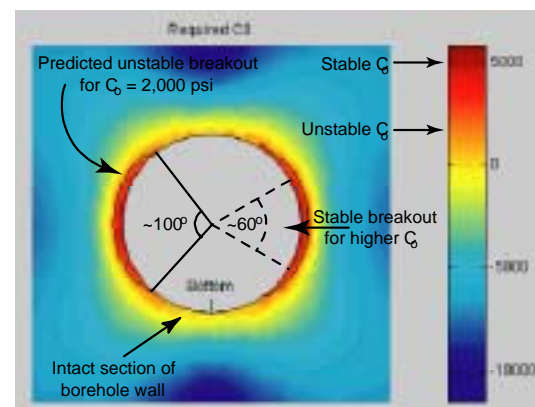


Figure 9. Output from the poroelastic analysis. The plot displays the horizontal borehole in cross section and the required rock strength ( $C_0$ —color coded) to maintain stability in and surrounding the well. The black line at the sides of the well shows the contour for  $C_0 = 2,000$  psi.

Tables

	$S_{hmin}$ [psi]	$S_v$ [psi]	$S_{Hmax}$ [psi]
Model 1	3,919	5,000	3,920
Model 2	3,919	5,000	5,277

Table 1. Stress magnitudes used for the dynamic wellbore stability analysis.

Case #	Reservoir status	$P_p$ [psi]	$dP$ [psi]	$dS/dP$	$S_{hmin}$ [psi]	$S_{Hmax}$ [psi]	$\nu$ [0.150 psi/c]	$\nu$ [0.150 psi/c]	Dryden [psi]	for $C_0 \geq 7,250$ psi	for $C_0 \geq 2,000$ psi
1	Initial condition	2475	0	0	3919	3920	= [0.150 psi/c]	39120	500	stable	fractured
2								39120	900	stable	fractured
3								39120	500	stable	fractured
4								1201300	500	stable	stable
5								39120	900	stable	stable
6								1201300	900	stable	stable
7	Depleted (I)	1875	500	0.75	3544	3545	= [0.150 psi/c]	39120	500	stable	stable
8								39120	900	stable	stable
9								39120	500	stable	stable
10								1201300	500	stable	stable
11								39120	900	stable	stable
12								1201300	900	stable	stable
13	Depleted (II)	1875	500	0.5	3469	3470	= [0.150 psi/c]	39120	500	stable	stable
14								39120	900	stable	stable
15								39120	500	stable	stable
16								1201300	500	stable	stable
17								39120	900	stable	stable
18								1201300	900	stable	stable
19	Depleted (III)	1475	1000	0.75	3163	3170	= [0.150 psi/c]	39120	500	stable	stable
20								39120	900	stable	stable
21								39120	500	stable	stable
22								1201300	500	stable	stable
23								39120	900	stable	stable
24								1201300	900	stable	stable
25	Depleted (IV)	1475	1000	0.5	3419	3420	= [0.150 psi/c]	39120	500	stable	stable
26								39120	900	stable	stable
27								39120	500	stable	stable
28								1201300	500	stable	stable
29								39120	900	stable	stable
30								1201300	900	stable	stable
31	Depleted (V)	975	500	0.75	2794	2795	= [0.150 psi/c]	39120	500	stable	stable
32								39120	900	fractured	stable
33								39120	500	stable	stable
34								1201300	500	stable	stable
35								39120	900	fractured	stable
36								1201300	900	fractured	stable
37	Depleted (VI)	975	500	0.5	3163	3170	= [0.150 psi/c]	39120	500	stable	stable
38								39120	900	fractured	stable
39								39120	500	stable	stable
40								1201300	500	stable	stable
41								39120	900	fractured	stable
42								1201300	900	fractured	stable
43	Depleted (VII)	475	2000	0.75	2419	2420	= [0.150 psi/c]	39120	500	fractured	stable
44								39120	900	fractured	stable
45								39120	500	fractured	stable
46								1201300	500	fractured	stable
47								39120	900	fractured	stable
48								1201300	900	fractured	stable
49	Depleted (VIII)	475	2000	0.5	2319	2320	= [0.150 psi/c]	39120	500	fractured	stable
50								39120	900	fractured	stable
51								39120	500	fractured	stable
52								1201300	500	fractured	stable
53								39120	900	fractured	stable
54								1201300	900	fractured	stable

Table 2. Parameters and results for the dynamic wellbore stability analysis.  $C_0$ : uniaxial compressive rock strength;  $P_p$ : pore pressure;  $dP$ : pore pressure depletion;  $dS/dP$ : change of stress with depletion as a result of poroelasticity.



